

DESIGN OF A WIDEBAND ESPAR ANTENNA FOR DVB-T RECEPTION

V. G. Tsiafakis, A. I. Sotiriou, Y. I. Petropoulos
E. S. Psarropoulos, E. D. Nanou, and C. N. Capsalis

Department of Electrical Engineering
Division of Information Transmission Systems
and Material Technology
National Technical University of Athens
9 Iroon Polytecneioy Str. 15772, Athens, Greece

Abstract—The design of an optimized Wideband Electronically Steerable Passive Array Radiator (W-ESPAR) antenna, for Terrestrial Digital Video Broadcasting (DVB-T) reception, is proposed. A genetic algorithm is used in order to calculate the positions and lengths of antenna elements (structural parameters) and loading conditions (control parameters). A nine-element W-ESPAR antenna with one element active and eight passive can have one directive beam per channel, with mean gain of 9 dBi, reflection factor less than 0.2 and input impedance around 75 Ohms. Computer simulations have shown that one main lobe may be achieved in the same direction and for all UHF channels, from 470 MHz to 890 MHz. The analytical results for the design are provided, and they show that the proposed W-ESPAR antenna is suitable for portable DVB-T reception.

1. INTRODUCTION

The explosive growth of Terrestrial Digital Video Broadcasting (DVB-T) is opening an enormous market with heterogeneous technical requirements. All countries that belong to geographic area Region 1 [1] have built their network digital plans during May and June of 2006 in Geneva at the Regional Radiocommunication Conference (RRC-06) [2]. Many of these countries have already begun their transition period from analogue to digital terrestrial television and some others are ready to start in order to complete the process before the deadline, June of

Corresponding author: V. G. Tsiafakis (vtsiaf@teemail.gr).

2015 [3]. Although the propagation conditions are the same for both analogue and digital transmission [4], the minimum E field required to achieve acceptable coverage is 3 to 20 dB higher for portable outdoor reception of a digital signal, depending on the system variant, whereas for portable indoor reception a maximum of 8 dB must be added [5].

Network operators are searching for new solutions that will provide broader bandwidth per user channel, better signal quality and improved Quality of Service (QoS) so that customers will take the advantages that DVB-T protocol offers. Even though many studies have proven that smart antenna technology may provide considerable benefits such as capacity increase, coverage increase and C/I improvement, their mass deployment is still weak [6–8]. High fabrication cost and complex configuration are the dominant factors that stall the installation of adaptive antenna systems. The cost increases with the number of radiator elements since the array needs the same number of RF high power amplifiers or low noise amplifiers. The same applies to digital beamforming antennas (DBF) due to the fact that D/A and A/D converters are needed for each element [9].

The concept of W-ESPAR antenna is based on the electronically steerable passive antenna array radiator (ESPAR) which is a loaded port adaptive antenna array, developed during the last few years. A typical ESPAR antenna is constructed from dipole elements without ground plane or from monopole elements with a ground plane. One element is active whereas the others are parasitic and have variable loads. The use of a circular ground plane of half wavelength radius with a skirt of a quarter wavelength that winds around it, can improve the horizontal angle of the peak directivity [10]. The simple configuration, small size and low fabrication cost, makes it an attractive solution for adaptive beamforming. A nine element ESPAR antenna has 9 dBi \pm 1 dB gain and null depth of -30 dBi \pm 10 dB for each direction and channel [11].

W-ESPAR has structural parameters identical to that of ESPAR. It consists of dipole elements without a ground plane, but can also be constructed with monopole elements with a ground plane (see Fig. 1). The parasitic elements are loaded with variable reactances which regulate the current in order to change the characteristics of the antenna, such as antenna diagram, directivity, gain, reflection factor and input impedance, according to the designer's needs.

The designed W-ESPAR antenna also exhibits beamforming capabilities. With the appropriate loading values, it is possible to have a slight steer of $\pm 15^\circ$ to the desirable reception direction. These capabilities are very important, especially in portable reception, where multipath phenomena change the signal's direction of arrival. A

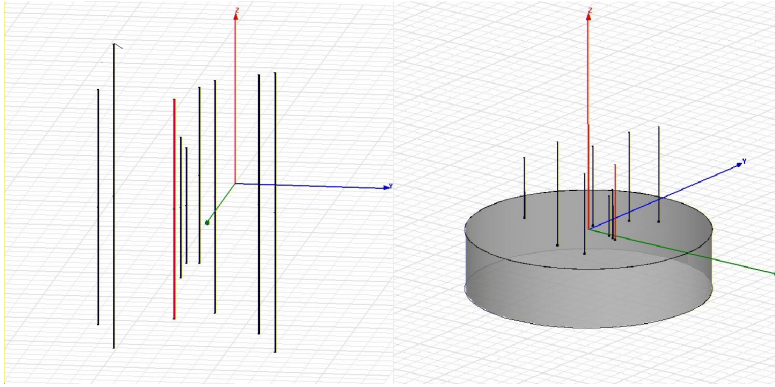


Figure 1. Wideband Electronically Steerable Passive Antenna Array Radiator (W-ESPAR) without and with ground plane and skirt.

common problem in portable reception is the need to manually correct the direction of the portable antenna when switching between television programs. W-ESPAR antenna can easily achieve this correction with an automatic change of the loading values.

In contrast to ESPAR, W-ESPAR has the advantage of being able to use the controlled loaded parasitic elements, to transform a narrowband antenna to a broadband one. ESPAR antennas are basically designed for wireless networks requiring a narrow spectrum [12] whereas the proposed W-ESPAR is designed to support broadcast applications covering radio frequencies of all UHF channels (21–69) [13].

2. THEORETICAL ANALYSIS

For an M-element antenna the voltage of the antenna is given by the following formula

$$\bar{V} = \bar{Z} \times \bar{I} \quad (1)$$

where \bar{V} is the voltage matrix, \bar{Z} is the impedance matrix and \bar{I} is the current matrix. Let x_i and i_i be the i -th element loading reactance and current, respectively. The transmitter impedance is defined as z_t and the transmitter voltage v_t [14]. The voltage of the transmitter and therefore of the central active element is normalized to 10 V.

$$v_i = 10 \text{ V} \quad (2)$$

The parasitic elements are connected to imaginary loads and no voltage is applied to them. Therefore

$$\overline{V_{par}(i)} = -\overline{I_{par}(i)} \times j \times \overline{X_{par}(i)} \quad (3)$$

where $\overline{V_{par}(i)}$ is the voltage matrix, $\overline{I_{par}(i)}$, the current matrix and $\overline{X_{par}(i)}$, the load matrix of the parasitic elements, $1 \leq i \leq M - 1$. Using Equations (1), (2) and (3) the system voltage can be expressed in matrix form as:

$$\overline{V} = \begin{bmatrix} v_t \\ 0 \\ 0 \\ \dots \\ \dots \\ 0 \end{bmatrix} - \begin{bmatrix} z_t & 0 & 0 & \dots & \dots & 0 \\ 0 & j * x_1 & 0 & \dots & \dots & 0 \\ 0 & 0 & j * x_2 & \dots & \dots & 0 \\ \dots & \dots & \dots & \dots & \dots & \dots \\ \dots & \dots & \dots & \dots & \dots & \dots \\ 0 & 0 & 0 & \dots & \dots & j * x_{M-1} \end{bmatrix} \begin{bmatrix} i_0 \\ i_1 \\ i_2 \\ \dots \\ \dots \\ i_{M-1} \end{bmatrix} \quad (4)$$

Defining \overline{V}_1 as the voltage matrix and Z_{diag} as the impedance matrix, Equation (4) can be written as:

$$\overline{V} = \overline{V}_1 - Z_{diag} * \overline{I} \quad (5)$$

From (1) and (5):

$$\overline{V}_1 - Z_{diag} * \overline{I} = \overline{Z} * \overline{I} \Leftrightarrow \overline{V}_1 = (\overline{Z} + Z_{diag}) * \overline{I} \quad (6)$$

and the current matrix \overline{I} can now be easily calculated.

Knowing the current flows, it is possible to evaluate the normalized radiation pattern, the maximum gain and the input impedance. The input impedance is given according to the following formula:

$$Z_{in} = \frac{v_t}{i_0} \quad (7)$$

The reflection coefficient is given by

$$\rho = \frac{Z_{in} - z_t}{Z_{in} + z_t} \quad (8)$$

where z_t is equal to 75Ω . The losses at the antenna input [15] are calculated by

$$loss = -10 * \log_{10}(1 - |\rho|^2)(dB) \quad (9)$$

where p is the absolute value of *coef*.

3. OPTIMIZATION STEPS

Optimization process was made in two phases. During the first phase, the desirable values for the maximum gain, input impedance and therefore reflection coefficient were set. A genetic algorithm (GA) [16, 17] was used in order to calculate the dimension, position and imaginary loads [18]. After several iterations the algorithm returned the characteristics of the antenna [19].

In our study, target gain, maximum accepted reflection coefficient and Z_0 were set to 11 dB, 0.2 and 75Ω , respectively. The optimization process was carried out by taking into account multiple frequencies, spread in the whole UHF spectrum: 471.25 MHz, 551.25 MHz, 631.25 MHz, 711.25 MHz, 791.25 MHz and 831.25 MHz. Mainly in Region 1 [1], UHF spectrum is separated in 49 channels of 8 MHz each (channel number 21–69). The selected frequencies were the vision frequencies per channel according to the PAL B, G system [13] in analog television.

The fitness function of the genetic algorithm, named error, is a linear combination of the normalized errors regarding the reflection coefficient and maximum gain. Defining:

$$error_target(f) = \left| \frac{p_target - p_calculated}{p_target} \right|^2 \quad (10)$$

$$error_gain(f) = \left| \frac{gain_target - gain_calculated}{gain_target} \right|^2 \quad (11)$$

where f is the frequency; p_target is the value for the desirable reflection coefficient; $p_calculated$ is the calculated value; $gain_target$ is the value for the desirable gain and $gain_calculated$ is the calculated value [20].

Since multiple frequencies were taken into consideration, the fitness function was determined by the following formula

$$error = \frac{\frac{1}{2} \left(\sum_{f=f_1}^{f_total} error_target(f) + \sum_{f=f_1}^{f_total} error_gain(f) \right)}{f_total} \quad (12)$$

where f_total is the number of frequencies selected for the simulation. The error function actually represents the mean value of two errors, gain and reflection coefficient. Using the mean value, both factors are treated equally by the algorithm.

For the design of the antenna, 20 individuals formed each generation of the GA. The initial ranges, from which the algorithm

entry values were chosen, are presented in Table 1. The genetic algorithm uses a uniform distribution for the selection of these values. Stochastic selection, scattered crossover with $p_{crossover} = 0.8$ and uniform mutation with rate equal to 0.2 were employed for the GA. Even though the imaginary loads were calculated during the first optimization stage, further optimization was considered necessary in order to enhance the antenna characteristics.

Table 1. Initial range for algorithm parameters.

| | Element Length | (x, y) Position | Imaginary Load |
|---------------|----------------|-------------------|----------------|
| Minimum value | 0.05 m | (-0.3 m, -0.3 m) | -250 j |
| Maximum value | 0.35 m | (0.3 m, 0.3 m) | 250 j |

During the second phase, the antenna structural parameters were kept the same as in the previous optimization phase. A new optimization took place regarding exclusively the loading values. Therefore, the input origin of the GA is only the values of the variable reactances [21]. The process was carried out for all UHF channels one by one. The second phase fitness function, $error_2$, follows Equation (12) where this time f_total is equal to unity because one frequency per optimization process is taken into consideration.

$$error_2 = \frac{error_target(f) + error_gain(f)}{2} \quad (13)$$

The algorithm parameters, initial range of the loads (-250 j to 250 j), stochastic selection, $p_{crossover} = 0.8$ and uniform mutation with rate equal to 0.2, were again employed.

4. SIMULATION PROCESS AND RESULTS

The design process was completed in four stages. During the first two stages, the simulation was performed according to the first phase of optimization, and took into account only one frequency at 631.25 MHz. In the first optimization phase, an eleven element antenna (one active, ten parasitic) was chosen. Further calculations during the second optimization phase, showed reflection coefficient values below 0.34 for frequencies from 550 MHz up to 740 MHz. For the rest of the spectrum, the values were significantly higher. The second attempt was made with a nine element antenna, having dipoles with double the radius compared to the dipoles of the previous case. The results were better regarding the lower spectrum frequencies, showing a reflection

coefficient value below 0.45 up to 710 MHz, but still not good enough for the upper frequencies.

In the third and final design stage, the simulation was performed according to the first optimization phase, taking into consideration more than one frequency. Splitting uniformly the UHF spectrum, the following frequencies were chosen: 471.25 MHz, 551.25 MHz, 631.25 MHz, 711.25 MHz, 791.25 MHz and 831.25 MHz. The third attempt was made with an eleven element antenna, and 2 mm radius for each element. The error function of the genetic algorithm was slightly different from Equation (12) and a weighting factor was assigned to the spectrum central frequency, $f = 631.25$ MHz with respect to the other frequencies. Although the reflection coefficient values were below 0.2, the gain presented significant fluctuations. The previous results lead to the final simulations set, where a nine element antenna with 2 mm element radius was chosen and the error function treated all the frequencies equally. Fig. 2 and Fig. 3 show the final antenna configuration, whereas Table 2 summarizes the antenna structural parameters.

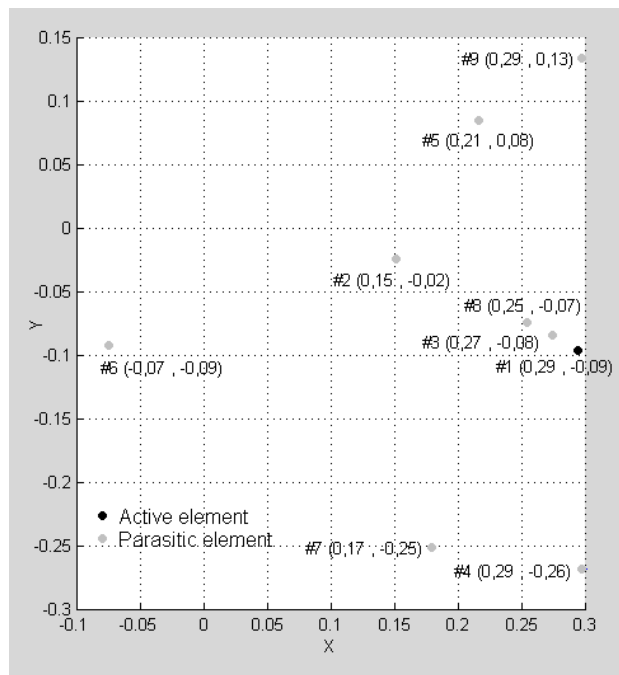


Figure 2. Designed wideband ESPAR antenna in the x - y plane.

After having determined the physical antenna configuration, one

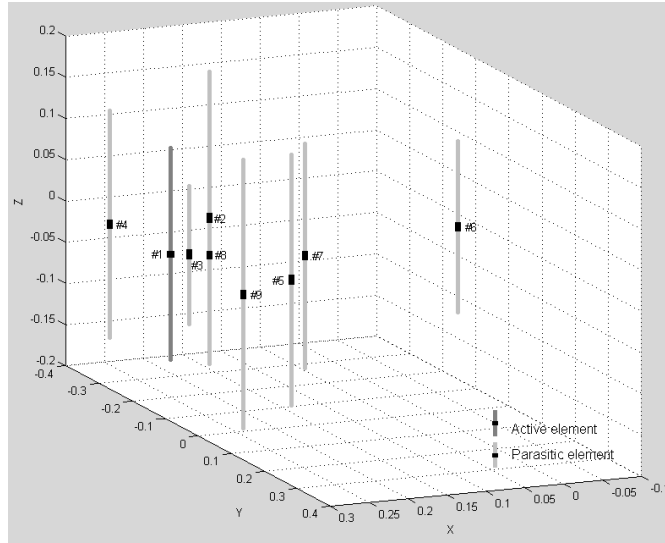


Figure 3. Designed wideband ESPAR antenna in the x - y - z plane.

Table 2. Structural parameters of the antenna.

| Element | Element Radius (m) | Element Length (m) | (x, y) Position |
|---------|--------------------|--------------------|--------------------|
| #1 | 0.002 | 0.25261 | 0.29441, -0.09581 |
| #2 | 0.002 | 0.26690 | 0.15156, -0.02453 |
| #3 | 0.002 | 0.16159 | 0.27550, -0.08404 |
| #4 | 0.002 | 0.26995 | 0.29922, -0.26796 |
| #5 | 0.002 | 0.29781 | 0.21579, 0.08535 |
| #6 | 0.002 | 0.20220 | -0.07384, -0.09320 |
| #7 | 0.002 | 0.34936 | 0.17811, -0.25096 |
| #8 | 0.002 | 0.13269 | 0.25410, -0.07396 |
| #9 | 0.002 | 0.32100 | 0.29808, 0.13437 |

simulation for each UHF channel has been implemented in order to calculate the loading values. Fig. 4 to Fig. 6 show the maximum antenna gain, the reflection coefficient and input impedance for each DVB-T channel and Table 3 and Table 4 summarize the parasitic elements loading values.

Figure 4 demonstrates the antenna gain for the whole UHF band which is relatively stable, without any deep fluctuations. The maximum value is 9.8259 dBi at 575.25 MHz and the minimum is equal

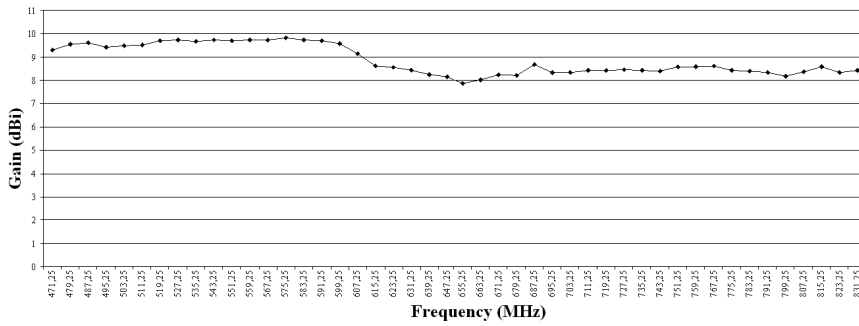


Figure 4. Gain of designed W-ESPAR antenna for frequencies from 471.25 MHz up to 831.25 MHz.

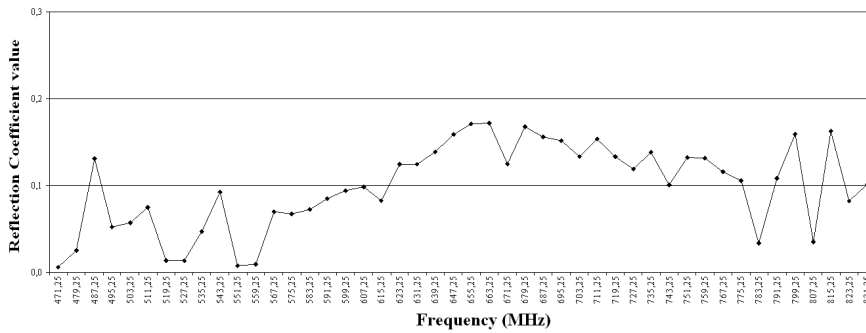


Figure 5. Reflection coefficient for frequencies from 471.25 MHz up to 831.25 MHz.

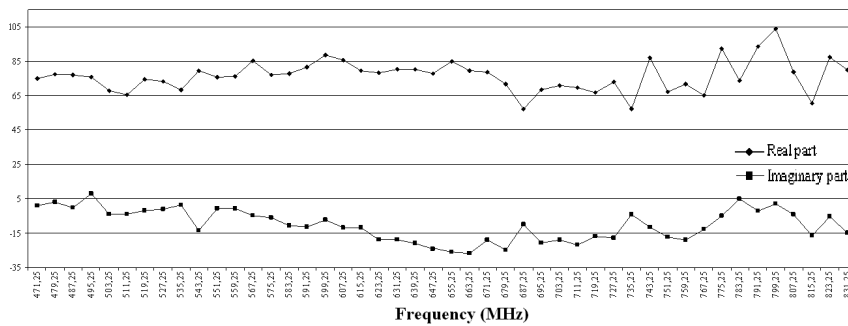


Figure 6. Z_{in} of designed W-ESPAR antenna for frequencies from 471.25 MHz up to 831.25 MHz.

to 7.8679 dBi at 655.25 MHz. Therefore, the maximum deviation is less than 2 dB and the antenna has an average gain of 9 dBi approximately. Fig. 5 presents the reflection coefficient variation. The maximum value appears at 663.25 MHz and is equal to 0.1721, a value that is 13.9% smaller than the target value of 0.2. The minimum reflection coefficient is 0.0056 at the 471.25 MHz. Next, Fig. 6 presents the antenna input impedance. Fig. 7 to Fig. 12 present the azimuth and elevation diagrams of the designed antenna for several radio frequencies.

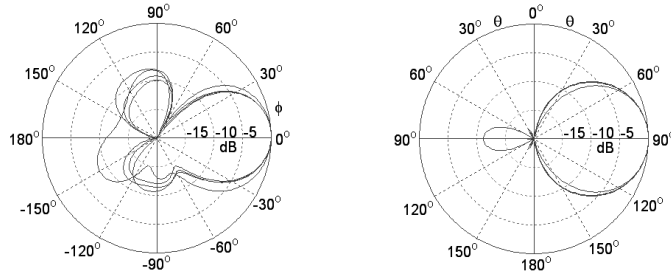


Figure 7. Radiation patterns for frequencies: 471.25 MHz, 487.25 MHz, 503.25 MHz and 519.25 MHz (azimuth plane & elevation plane).

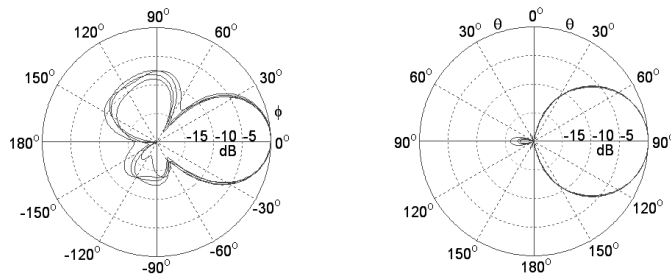


Figure 8. Radiation patterns for frequencies: 535.25 MHz, 551.25 MHz, 567.25 MHz and 583.25 MHz (azimuth plane & elevation plane).

Having determined the physical antenna configuration and the loading values for each UHF channel, one last simulation has been implemented in order to achieve beamforming capabilities [22]. With specific loading values, it is possible to achieve a slight steer of the desirable reception angle. Simulation results have shown that instead

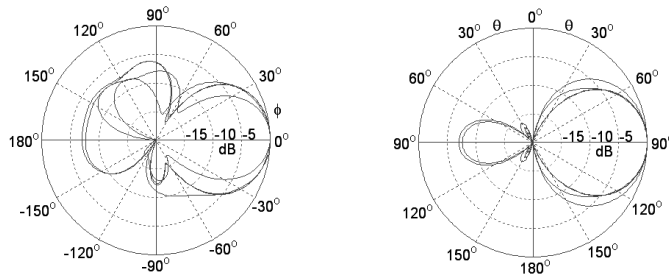
Table 3. (a) Imaginary loads of parasitic elements.

| Frequency (MHz) | Va1 | Va2 | Va3 | Va4 | Va5 | Va6 | Va7 | Va8 |
|--------------------|--------|--------|-------|--------|-------|--------|--------|--------|
| 471.25 | 55 j | 290 j | 174 j | -2 j | 212 j | -122 j | 39 j | 152 j |
| 479.25 | 35 j | 280 j | 299 j | -2 j | 207 j | -130 j | 137 j | -125 j |
| 487.25 | 14 j | 277 j | 288 j | -12 j | 209 j | -130 j | 141 j | -101 j |
| 495.25 | 14 j | 245 j | 290 j | -32 j | 185 j | -169 j | 261 j | -238 j |
| 503.25 | -6 j | 267 j | 294 j | -43 j | 205 j | -149 j | 154 j | -100 j |
| 511.25 | -18 j | 285 j | 284 j | -55 j | 191 j | -166 j | -296 j | -112 j |
| 519.25 | -40 j | 266 j | 299 j | -62 j | 177 j | -188 j | 121 j | -150 j |
| 527.25 | -51 j | 275 j | 299 j | -76 j | 168 j | -105 j | 76 j | -161 j |
| 535.25 | -60 j | 271 j | 255 j | -89 j | 151 j | -226 j | 120 j | -191 j |
| 543.25 | -96 j | -291 j | 286 j | -99 j | 154 j | -248 j | -297 j | -202 j |
| 551.25 | -91 j | -146 j | 295 j | -120 j | 138 j | -256 j | -63 j | -205 j |
| 559.25 | -108 j | 76 j | 290 j | -131 j | 124 j | -288 j | -178 j | -240 j |
| 567.25 | -140 j | 85 j | 294 j | -149 j | 131 j | -294 j | 234 j | -230 j |
| 575.25 | -157 j | 130 j | 290 j | -157 j | 117 j | -296 j | 279 j | -266 j |
| 583.25 | -178 j | 144 j | 206 j | -177 j | 105 j | -297 j | 250 j | -290 j |
| 591.25 | -213 j | 136 j | 296 j | -191 j | 105 j | -298 j | 252 j | -290 j |
| 599.25 | -237 j | 131 j | 296 j | -213 j | 94 j | -299 j | 254 j | -298 j |
| 607.25 | -251 j | 143 j | 161 j | -249 j | 86 j | -295 j | 185 j | -299 j |
| 615.25 | -194 j | 146 j | 188 j | -263 j | 59 j | -298 j | 180 j | 299 j |
| 623.25 | -223 j | 139 j | 153 j | -282 j | 52 j | -299 j | 193 j | 291 j |
| 631.25 | -231 j | 136 j | 188 j | -299 j | 40 j | -299 j | 181 j | 294 j |
| 639.25 | -222 j | 134 j | 299 j | -296 j | 25 j | -295 j | 147 j | 297 j |
| 647.25 | -110 j | -299 j | 211 j | -45 j | 159 j | -299 j | 207 j | -23 j |
| 655.25 | -32 j | 106 j | 137 j | -147 j | 72 j | -299 j | 131 j | -78 j |
| 663.25 | -75 j | 105 j | 178 j | -65 j | 76 j | -299 j | 259 j | -35 j |
| 671.25 | -172 j | 120 j | 166 j | 295 j | -69 j | -298 j | 194 j | -84 j |
| 679.25 | -127 j | 99 j | 121 j | -69 j | 56 j | -294 j | 196 j | -82 j |
| 687.25 | -203 j | 96 j | 151 j | 298 j | -16 j | -299 j | 178 j | 112 j |
| 695.25 | -175 j | 91 j | 121 j | -25 j | 39 j | -297 j | 182 j | -107 j |
| 703.25 | -191 j | 86 j | 77 j | -11 j | 28 j | -277 j | 188 j | -101 j |

of having maximum gain at 0 degree, the main lobe may be directed to an angle of $\pm 15^\circ$. The gain as well as input impedance and reflection factor remain in the same range. Fig. 13 and Fig. 14 present the results of azimuth and elevation diagrams, showing a maximum reception gain

Table 4. (b) Imaginary loads of parasitic elements.

| Frequency (MHz) | Va1 | Va2 | Va3 | Va4 | Va5 | Va6 | Va7 | Va8 |
|-----------------|--------|------|-------|-------|--------|--------|-------|--------|
| 711.25 | -249 j | 83 j | 89 j | 297 j | -87 j | -295 j | 169 j | -137 j |
| 719.25 | -215 j | 77 j | 66 j | 50 j | 1 j | -292 j | 171 j | -73 j |
| 727.25 | -233 j | 71 j | 52 j | 62 j | -5 j | -299 j | 172 j | -105 j |
| 735.25 | -268 j | 71 j | 109 j | 68 j | -13 j | -286 j | 162 j | -132 j |
| 743.25 | -272 j | 59 j | 48 j | 104 j | -7 j | -291 j | 186 j | -104 j |
| 751.25 | -285 j | 60 j | 61 j | 169 j | -41 j | -299 j | 155 j | -156 j |
| 759.25 | -291 j | 55 j | 50 j | 212 j | -59 j | -298 j | 152 j | -173 j |
| 767.25 | -299 j | 52 j | 42 j | 173 j | -64 j | -292 j | 147 j | -135 j |
| 775.25 | -297 j | 42 j | 11 j | 135 j | -81 j | -289 j | 158 j | -143 j |
| 783.25 | -299 j | 42 j | -29 j | 58 j | -130 j | -287 j | 148 j | -298 j |
| 791.25 | -296 j | 35 j | -7 j | 78 j | -110 j | -299 j | 147 j | -9 j |
| 799.25 | -299 j | 29 j | -37 j | 25 j | -133 j | -299 j | 147 j | -40 j |
| 807.25 | -281 j | 31 j | -39 j | 4 j | -143 j | -281 j | 132 j | 56 j |
| 815.25 | -299 j | 30 j | -29 j | 167 j | -160 j | -299 j | 123 j | 21 j |
| 823.25 | -300 j | 22 j | -55 j | -1 j | -188 j | -299 j | 126 j | 79 j |
| 831.25 | -300 j | 20 j | -65 j | 21 j | -212 j | -299 j | 120 j | 127 j |

**Figure 9.** Radiation patterns for frequencies: 599.25 MHz, 615.25 MHz, 631.25 MHz and 647.25 MHz (azimuth plane & elevation plane).

at $+15^\circ$ and -15° respectively, for frequency equal to 531.25 MHz. Table 5 summarizes the antenna characteristics for the above two cases. In order to verify the results concerning the maximum gain of the antenna, a simulation using the software package HFSS was made.

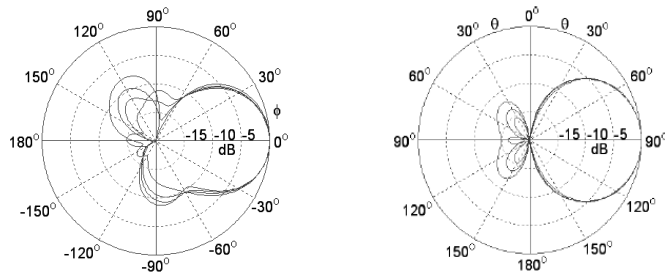


Figure 10. Radiation patterns for frequencies: 663.25 MHz, 679.25 MHz, 695.25 MHz and 711.25 MHz (azimuth plane & elevation plane).

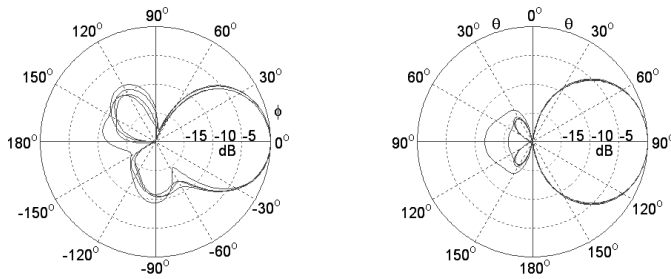


Figure 11. Radiation patterns for frequencies: 727.25 MHz, 743.25 MHz, 759.25 MHz and 775.25 MHz (azimuth plane & elevation plane).

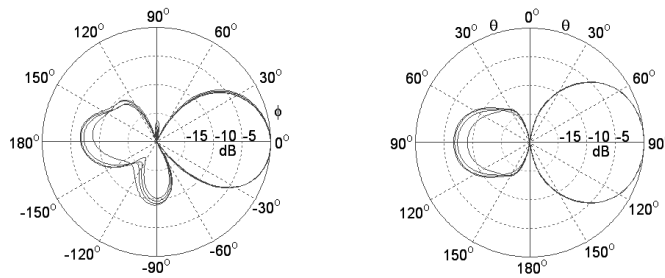


Figure 12. Radiation patterns for frequencies: 791.25 MHz, 807.25 MHz, 823.25 MHz and 831.25 MHz (azimuth plane & elevation plane).

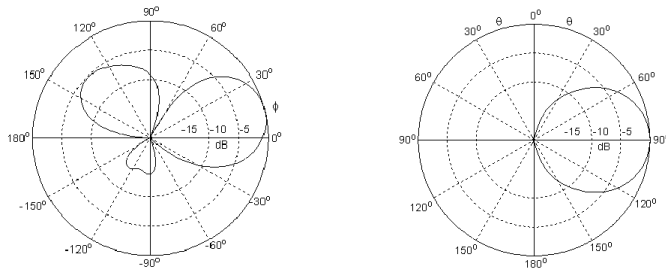


Figure 13. Radiation pattern with maximum reception gain at $+15^\circ$ for 531.25 MHz (azimuth plane & elevation plane).

Table 5. Parameters of the antenna for different maximum direction gain.

| | | | | | | | |
|-----------------------------------|-------|-------------|--------|-------|--------|-------|------|
| Direction of Maximum Antenna Gain | | $+15^\circ$ | | | | | |
| Maximum Antenna Gain Value | | 9.6 dBi | | | | | |
| Reflection Coefficient | | 0.096 | | | | | |
| Imaginary Loads | | | | | | | |
| VA1 | VA2 | VA3 | VA4 | VA5 | VA6 | VA7 | VA8 |
| -66 j | -22 j | 64 j | -126 j | 137 j | -200 j | 84 j | -179 |
| Direction of Maximum Antenna Gain | | -15° | | | | | |
| Maximum Antenna Gain Value | | 8.4 dBi | | | | | |
| Reflection Coefficient | | 0.1078 | | | | | |
| Imaginary Loads | | | | | | | |
| VA1 | VA2 | VA3 | VA4 | VA5 | VA6 | VA7 | VA8 |
| -11 j | 171 j | 197 j | -132 j | 112 j | -199 j | 198 j | -156 |

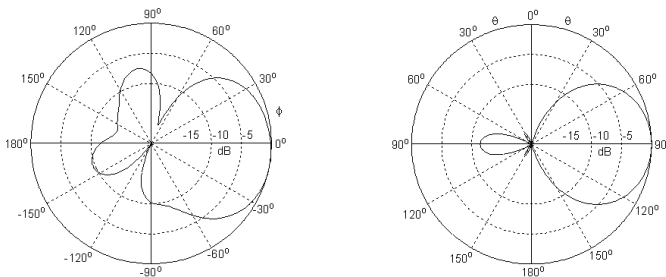


Figure 14. Radiation pattern with maximum reception gain at -15° for 531.25 MHz (azimuth plane & elevation plane).

The calculations were made for the frequencies 471.25, 655.25, 743.25 and 799.25 MHz and the corresponding values of the maximum gain are 8.61, 8.6, 8.36 and 6.35. The comparison between these values and the values of our analysis showed a small variation which verifies the consistency of the results of our study.

5. CONCLUSIONS

The proposed W-ESPAR antenna is a wideband antenna with one steerable directive beam, mean gain of 9 dBi and reflection factor less than 0.2, using parasitic elements that are loaded with variable reactances.

In this paper, a genetic algorithm was used in two phases. In the first phase the structural characteristics of the antenna were defined. Due to time and computing limitations, only six vision frequencies, corresponding to the channels 21, 31, 41, 51, 61 and 66 in the UHF band, were used. In the second phase the values of the variable loads were calculated. The calculations were made for each UHF channel.

The algorithm was set to achieve not only good characteristics of the antenna in all UHF channels, but also steerable capabilities. An electronic steer range of $30^\circ(-15^\circ, +15^\circ)$ was accomplished with specific values for the variable loads on each occasion. For all optimization phases, 20 individuals formed each generation of the GA. With a larger population, the algorithm would search a wider solution space but with much slower rate.

In ESPAR antenna, adaptive radiation characteristics are provided by controlling the current in the variable reactances. On the contrary, W-ESPAR antenna uses the variable reactances in order to achieve stable antenna gain and reflection factor in whole UHF band (approximate bandwidth of 400 MHz) and a slight steer of the directive beam. The dimensions of W-ESPAR antenna ($40 \times 50 \times 34$ cm) make it suitable for domestic use, for fixed and portable indoor reception of analogue and digital terrestrial television. The antenna design in the current study considers dipole elements without ground plane. Like ESPAR antennas, the proposed W-ESPAR may be implemented with monopole elements and a ground plane. This is going to reduce the height of the antenna structure and make it more stable.

W-ESPAR is not probably the appropriate name for this antenna, mainly because it is not fully steerable, even though the complete design of the structure, the use of the variable reactances and the steer of the directive beam for at least 30° explain the selection of the name. This approach of antenna designing provides portable solutions for fixed, portable indoor and outdoor reception for both analogue and

digital television.

In terrestrial television, broadcasters use more than one transmitter in order to cover big cities or areas where the required field strength is not achieved. Normally, users have the experience to orient the antenna and achieve better image quality. The proposed W-ESPAR antenna gives users the capability to accomplish better signal quality and an automatic orientation of the antenna when switching between television channels.

REFERENCES

1. International Telecommunication Union, *Radio Regulations*, Edition of 2007.
2. International Telecommunication Union, *Final Acts of the Regional Radiocommunication Conference for Planning of the Digital Terrestrial Broadcasting Service in Parts of Regions 1 and 3 in the Frequency Bands 174–230 MHz and 470–862 MHz (RRC-06)*, Geneva, 2006.
3. International Telecommunication Union, *Final Acts of the Regional Radiocommunication Conference for the Revision of the Stockholm 1961 Agreement (RRC-06-Rev.ST61)*, Geneva, 2006.
4. European Conference of Postal and Telecommunications Administrations, *The Chester 1997 Multilateral Coordination Agreement Relating to Technical Criteria, Coordination Principles and Procedures for the Introduction of Terrestrial Digital Video Broadcasting (DVB-T)*, Chester, July 25, 1997.
5. International Telecommunication Union, *DTTB Handbook Digital Terrestrial Television Broadcasting in the VHF/UHF Bands*, Radiocommunication Bureau Edition, 2002.
6. Lozano, A., F. R. Farrokhi, and R. A. Valenzuela, “Lifting the limits on high-speed wireless data access using antenna arrays,” *Communications Magazine*, Vol. 39, No. 9, 156–162, September 2001.
7. Herscovici, N. and C. Chrostodoulou, “Why have smart antennas not yet gained any traction with wireless network operators,” *IEEE Antennas and Propagation Magazine*, Vol. 47, No. 6, December 2005.
8. Lehne, P. H. and M. Pettersen, “An overview of smart antenna technology for mobile communication systems,” *IEEE Communications Surveys*, Vol. 2, No. 4, 2–13, Fourth Quarter, 1999.
9. Liberti, J. C. and T. S. Rappaport, *Smart Antennas for*

Wireless Communication: IS-95 and Third Generation CDMA Applications, Prentice Hall, 1999.

10. Gyoda, K. and T. Ohira, "Electronically steerable passive array radiator antennas for low-cost analog adaptive beamforming," *Proc. 2000 IEEE International Conference on Phased Array Systems and Technology*, 101–104, 2000.
11. Kawakami, H. and T. Ohira, "Electronically Steerable Passive Array Radiator (ESPAR) antennas," *IEEE Antennas and Propagation Magazine*, Vol. 47, No. 2, April 2005.
12. Gyoda, K. and T. Ohira, "Design of Electronically Steerable Passive Array Radiator (ESPAR) antennas," *2000 IEEE Antennas and Propagation Society International Symposium*, 922–925, 2000.
13. International Telecommunication Union, *Final Acts of the European Broadcasting Conference in the VHF and UHF Bands*, Stockholm, 1961.
14. Capsalis, C. and P. Kottis, *Keraies Asyrmates Zefkseis*, Tziolas Editions, Athens, Greece, 2007.
15. Balanis, C. A., *Antenna Theory Analysis and Design*, John Wiley & Sons, 2005.
16. Goldberg, D. E., *Genetic Algorithms in Search, Optimization, and Machine Learning*, Addison-Wesley, 1989.
17. Rahmat-Samii, Y. and E. Michielssen, *Electromagnetic Optimization by Genetic Algorithms*, John Wiley & Sons Inc., 1999.
18. Sijher, T. S. and A. A. Kishk, "Antenna modeling by infinitesimal dipoles using genetic algorithms," *Progress In Electromagnetics Research*, PIER 52, 225–254, 2005.
19. Meng, Z.-Q., "Autonomous genetic algorithm for functional optimization," *Progress In Electromagnetics Research*, PIER 72, 253–268, 2007.
20. Orchard, B., *Optimizing Algorithms for Antenna Design*, M.Sc. Dissertation, University of the Witwatersrand, 2002.
21. Mitilineos, S. A., C. A. Papagianni, G. I. Verikaki, and C. N. Capsalis, "Design of switched beam planar array using the method of genetic algorithms," *Progress In Electromagnetics Research*, PIER 46, 105–126, 2004.
22. Lee, K.-C., "A genetic algorithm based direction finding technique with compensation of mutual coupling effects," *Journal of Electromagnetic Waves and Applications*, Vol. 17, No. 11, 1613–1624, 2003.